

## UC Davis

### UC Davis Previously Published Works

#### Title

Use of variogram analysis to classify field peas with and without internal defects caused by weevil infestation

#### Permalink

<https://escholarship.org/uc/item/1kp646k9>

#### Authors

Nansen, Christian  
Zhang, Xuechen  
Aryamanesh, Nader  
[et al.](#)

#### Publication Date

2014-02-01

#### DOI

10.1016/j.jfoodeng.2013.09.001

Peer reviewed

Provided for non-commercial research and education use.  
Not for reproduction, distribution or commercial use.



This article appeared in a journal published by Elsevier. The attached copy is furnished to the author for internal non-commercial research and education use, including for instruction at the authors institution and sharing with colleagues.

Other uses, including reproduction and distribution, or selling or licensing copies, or posting to personal, institutional or third party websites are prohibited.

In most cases authors are permitted to post their version of the article (e.g. in Word or Tex form) to their personal website or institutional repository. Authors requiring further information regarding Elsevier's archiving and manuscript policies are encouraged to visit:

<http://www.elsevier.com/authorsrights>

Contents lists available at [ScienceDirect](http://www.sciencedirect.com)

## Journal of Food Engineering

journal homepage: [www.elsevier.com/locate/jfoodeng](http://www.elsevier.com/locate/jfoodeng)

# Use of variogram analysis to classify field peas with and without internal defects caused by weevil infestation

Christian Nansen<sup>a,c,\*</sup>, Xuechen Zhang<sup>a,b,c</sup>, Nader Aryamanesh<sup>b,c</sup>, Guijun Yan<sup>b,c</sup><sup>a</sup>School of Animal Biology, Faculty of Science, The University of Western Australia, 35 Stirling Highway, Crawley, Perth, Western Australia 6009, Australia<sup>b</sup>School of Plant Biology, Faculty of Science, The University of Western Australia, 35 Stirling Highway, Crawley, Perth, Western Australia 6009, Australia<sup>c</sup>The UWA Institute of Agriculture, The University of Western Australia, 35 Stirling Highway, Crawley, Perth, Western Australia 6009, Australia

## ARTICLE INFO

## Article history:

Received 29 January 2013

Received in revised form 11 August 2013

Accepted 2 September 2013

Available online 11 September 2013

## Keywords:

Hyperspectral imaging

Field peas (*Pisum sativum*)Pea weevil (*Bruchus pisorum*)

Quality control

Variogram analysis

Classification sensitivity and specificity

## ABSTRACT

In this study, we acquired 72 (training data) and 30 (independent validation) high-spatial resolution (7 by 7 pixels per mm<sup>2</sup>) hyperspectral imaging data [240 spectral bands from 392 to 889 nm (spectral resolution = 2.1 nm)] from samples of field peas (*Pisum sativum*) with and without pea weevil (*Bruchus pisorum*) infestation. The reflectance data were analyzed with linear discriminant analysis (LDA) or either reflectance values only or of a combination of reflectance values and variogram parameters (derived from variogram analysis) from a single spectral band (782 nm). All examined classification models were assessed based on sensitivity (ability to positively detect infestation), specificity (ability to positively detect non-infestation), and accurate classification of 30 samples of independent validation data. Highest classification performance was obtained with a combination of reflectance values in two spectral bands (641 nm and 868 nm) and variogram parameters derived from 782 nm. This classification model was associated with a sensitivity of 94.7% and a specificity of 100%. In addition, all 30 independent validation data were accurately classified (100%). For comparison, traditional linear discriminant analyses of 108,351 reflectance profiles from individual pixels in the 72 samples or average reflectance profiles from the 72 samples classified the validation data with 84.0% and 83.3% accuracy, respectively. We are unaware of any reflectance-based classification system, which – based on reflectance data acquired in only three channels (spectral bands) – can provide this level of sensitivity and specificity and classification of independent validation data of internal defects in food products. Accurate and reliable classification of food objects based reflectance values in only a few spectral bands would likely imply low computer processing requirements and rapid data analysis. Thus, we believe that the current classification method may be useful for quality control systems of a wide range of food products.

© 2013 Elsevier Ltd. All rights reserved.

## 1. Introduction

Hyperspectral imaging technology has been used widely in detection of food defects (Kong et al., 2004), assessment of food quality (Ariana and Renfu, 2010; Fontaine et al., 2002; Lu and Peng, 2006; Martens and Martens, 1986; Okamoto and Lee, 2009), classification of near-isogenic crop genotypes (Nansen et al., 2008), and in detection of surface contaminations (Lefcote and Kim, 2006; Mehl et al., 2004; Park et al., 2006; Vargas et al., 2005). Comprehensive reviews of the use of imaging technology in detection of traits in food products have been published (Gowen et al., 2007; Wang and Paliwal, 2007). Despite a large bulk of research supporting the concept of using reflectance-based technologies in classification

of food products, there are important challenges, which justify continued research into improved classification methods. Many unprocessed food products (i.e. apples, potatoes, peaches, nuts, and seeds) vary considerably both within each object and between objects (i.e. varieties) in terms of color, size and shape. This physical variability in object characteristics (i.e. background color) represents a considerable challenge, when the objective is to develop reflectance-based classifiers to be used for accurate detection and/or characterization of quality traits in food products (ElMasry et al., 2008; Okamoto and Lee, 2009). We argue that classification challenges imposed by physical variability in object characteristics are exacerbated by the fact that most classification methods are based on the fundamental assumption that reflectance values in selected narrow spectral bands can be used to identify objects (food items) with/without certain quality traits or with traits ranging along a continuous gradient. That is, either through spectral band ratios or coefficients, it is the relative relationship between reflectance values in different spectral bands that determine whether a pixel or the average reflectance profile of an object is

\* Corresponding author. Address: The University of Western Australia, School of Animal Biology, The UWA Institute of Agriculture, 35 Stirling Highway, Crawley, Perth, Western Australia 6009, Australia. Tel.: +61 (0) 8 6488 4717; fax: +61 (0) 8 6488 7354.

E-mail address: [christian.nansen@uwa.edu.au](mailto:christian.nansen@uwa.edu.au) (C. Nansen).

classified as “a” or “b”. Linear discriminant analysis (Fisher, 1936) has been used successfully in many hyperspectral image based classifications of food products (Park et al., 2007; Gcdmez-Sanchis et al., 2008; Nansen et al., 2008; Gowen et al., 2009; Liu et al., 2010; Kalkan et al., 2011; Shahin and Symons, 2011). An alternative classification approach is possible, when hyperspectral imaging data are acquired, because each pixel is associated with a relative coordinate ( $x$  and  $y$ ) within the image cube (Nansen, 2012). Consequently, it is possible to characterize the spatial structure of reflectance values in a single spectral band (using variogram analysis) and determine to what extent a given quality trait of the target object is associated with a particular spatial data structure. While use of variogram analysis is well-described in geosciences, landscape ecology, oceanography, and other large-scale life science applications, it is only recently that this approach has been applied to high-resolution hyperspectral imaging data (Nansen, 2011, 2012; Nansen et al., 2010a; Nansen et al., 2009). The assumption behind variogram-based analysis is that the spatial structure of reflectance values in individual spectral bands can be described by three fitted variogram parameters, and that these variogram parameters vary significantly among classes of target objects. For example, if food products possess: (1) surface residues (chemical residues or other contaminations), (2) bruised or surface damaged surfaces, or (3) internal defects that markedly alter the reflectance in portions of a given food product – then it seems reasonable to assume that the relationship between reflectance values in adjacent pixels (and therefore the spatial structure of reflectance values in individual spectral bands) changes.

In this study, we tested the hypothesis that fitted variogram parameters derived from reflectance data of field peas (*Pisum sativum*) can be used effectively in combination with average reflectance values to accurately detect pea weevil infestation (*Bruchus pisorum*). The 24 (12 varieties with/without pea weevil infestation) field pea samples included in this study represented a wide range of background colors ranging across golden, red, and dark brown (Fig. 1), so this data set was considered very suitable for the challenge of detecting a consistent reflectance response to pea weevil infestation. In addition to developing accurate classification methods, it is also important that classification models have low computer processing requirements, as that increases classification speed and reduces costs of implementing image based classification systems in the food industry and elsewhere.

## 2. Materials and methods

### 2.1. Hyperspectral imaging data

The pea samples were produced by Byrne et al. (2008) and advanced further by Aryamanesh et al., (2012). Seven pea weevil resistance field pea backcross lines (BC1F6), introgressed from *P. fulvum* into cultivated field pea through backcrossing were selected. Five field pea cultivars, mainly for human food, including Pennant, Dunwa, Kaspas, Yarrum and Helena were also included in this experiment. Recently, Aryamanesh et al. (2012) developed a quick and reliable method to screen pea weevil infestation under field trial conditions, using a density separation selection method with caesium chloride (CsCl). However, field peas subjected to CsCl-based evaluation of pea weevil infestation are not available for human consumption due to health concerns associated with CsCl residues. Individual peas were selected based on careful visual inspection and a novel CsCl based density separation method to differentiate field peas with or without pea weevil infestation (Aryamanesh et al., 2012). Field peas were divided into infested and non-infested classes. For each of the 24 classes (12 pea samples with/without weevil infestation), 3–10 individual peas were

imaged with three replications for each class (new peas each time) (Fig. 1). Thus, a total of 72 hyperspectral images comprised the training data set. For independent validation of the proposed classification model, additional hyperspectral images were acquired from five (Pennant, Dunwa, Helena, Kaspas, and Yarrum) of the used field pea samples (5 samples  $\times$  with/without pea weevil infestation  $\times$  3 replications,  $N = 30$ ) on a separate day. The variation in number of individual field peas was due to scarcity of field peas in some of the classes, but they were included to increase the diversity of background colors.

Similar to methodology used in previously published studies (Nansen et al., 2010a; Nansen et al., 2010b), we used a hyperspectral spectral camera (PIKA II, Resonon Inc., Bozeman, MT) mounted 40 cm above target objects (field peas). The main specifications of the spectral camera are as follows: interface, Firewire (IEEE 1394b); output, digital (12 bit); 240 bands from 392 to 889 nm (spectral resolution = 2.1 nm) (spectral) by 640 pixels (spatial); angular field of view of 7°. The objective lens had a 35 mm focal length (maximum aperture of F1.4), optimized for the near-infrared and visible near-infrared spectra. Hyperspectral images were collected with artificial lighting from 15 W, two 12 V LED light bulbs mounted on either side of the lens in a room with 19–22 °C temperature and 30–40% relative humidity. Reflectance data were acquired with the spatial resolution of 7 by 7 pixels per mm<sup>2</sup>. A piece of white Teflon (K-Mac Plastics, MI, USA) was used for white calibration, and “relative reflectance” was referred to proportional reflectance compared to reflectance obtained from Teflon. Each hyperspectral image cube consisted of 100 frames (64,000 pixels), and relative reflectance values ranged between 0 and 1. Colored plastic cards (green, yellow, and red) were imaged at imaging event and average reflectance profiles from these cards were used to confirm high consistency of hyperspectral image acquisition conditions (less than 2% variance in individual spectral bands).

### 2.2. Data processing and analysis

A customized software package was used to spatially average (in  $5 \times 5$  pixel grids) reflectance profiles and convert hyperspectral image files in BIL-format into txt-files. All data processing and analysis were subsequently conducted in PC-SAS 9.3 (SAS Institute, NC). With three replicated images of each of the 24 field pea classes, a training data based on reflectance data from 72 hyperspectral images was used to develop a classification model. The first step in the analysis consisted of reducing the amount of input data and also reduce within class variation by excluding pixels (reflectance profiles), which were considered to represent noise (i.e. white background, shadows, and reflectance data from pea weevil exit holes in individual field peas). These pixels were excluded by applying a radiometric filter (Eq. (1)), so that reflectance profiles (pixels) were only included, if the relative reflection values in three spectral bands (R430, R480, and R800) were:

$$R430 < 0.15 \text{ and } R480 < 0.35 \text{ and } R800 > 0.30 \quad (1)$$

After this spatial data reduction, the training data set from the 72 field pea samples consisted of 108,351 reflectance profiles. The second step in the analysis consisted of spectral data reduction by identifying the 20 spectral bands with highest contribution to the classification of reflectance profiles from weevil infested (INF = 1) and non-infested (INF = 0) field peas. Linear discriminant analysis (LDA) (Fisher, 1936) has been used widely in classifications of food products based on hyperspectral imaging (Park et al., 2007; Gcdmez-Sanchis et al., 2008; Nansen et al., 2008; Gowen et al., 2009; Liu et al., 2010; Kalkan et al., 2011; Shahin and Symons, 2011; Baranowski et al., 2012). Consequently, stepwise LDA (PROC STEPDISC) was used to select the “best” 20 spectral



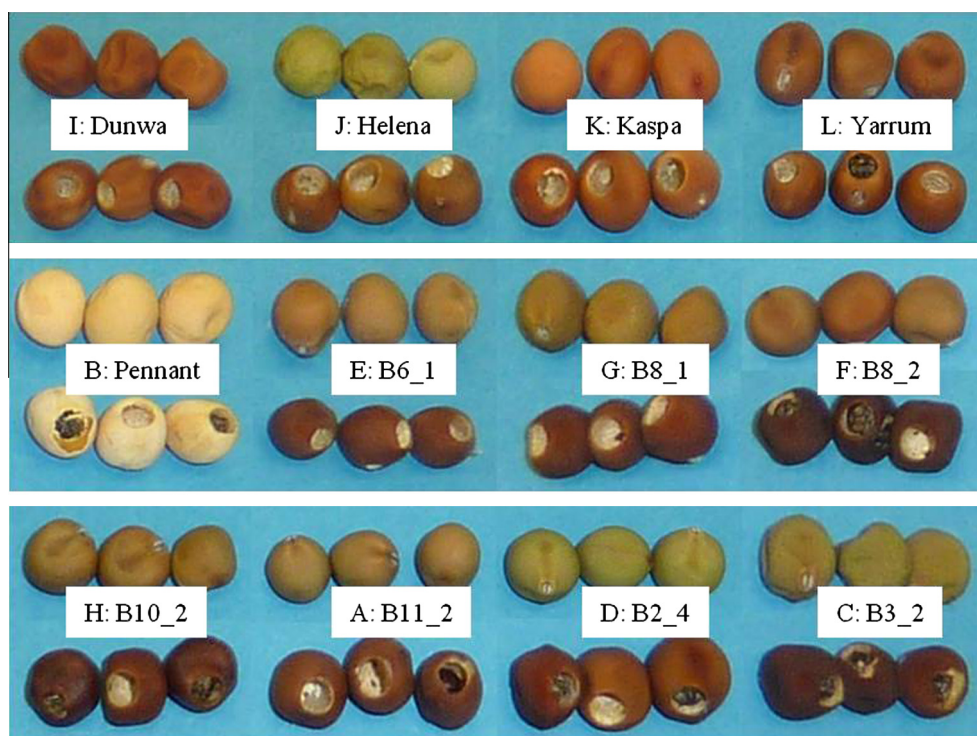


Fig. 1. Photos of the 12 field pea samples included in this study with non-infested in top and weevil infested in bottom rows.

bands. Only these 20 spectral bands (out of 240 spectral bands) were considered further. Subsequently, we conducted two traditional linear LDAs (PROC DISCRIM option = crossvalidate) of: (1) all included pixels from field pea samples ( $N = 108,351$  reflectance profiles), and (2) average reflectance profiles from each of the field pea samples ( $N = 72$  reflectance profiles). In addition, we conducted two LDAs, in which variogram parameters (see below) derived from a single spectral band (782 nm) were used either alone or in combination with average reflectance values as explanatory variables. The spectral band at 782 nm was chosen, as the initial stepwise LDA indicated that it was the spectral band which contributed the most to the separation of infested and non-infested pea samples.

Spatial structure analysis based on geostatistics (variogram analysis) is considered one of the most powerful and robust approaches to spatial data analysis (Isaaks and Srivastava, 1989), and recent studies have shown how variogram parameters derived from high-resolution reflectance data can be used to detect different traits in a range of target objects (Nansen, 2011, 2012; Nansen et al., 2010a; Nansen et al., 2010b; Nansen et al., 2009; Nansen et al., 2010c). In the variogram analysis (PROC VARIOGRAM) of reflectance data at 782 nm, we used the following variogram settings: (1) lag distances = 1, and (2) number of lag intervals = 10. The following regression fit (PROC NLIN) was used to generate variogram coefficients for each of the 72 hyperspectral images:

$$F(D) = a + b(1 - e^{(-c \times D)}) \quad (2)$$

In which  $a$ ,  $b$ , and  $c$  are fitted coefficients and  $D$  denotes the lag distance and  $F(D)$  is the semi-variance at lag distance,  $D$ . Although other regression fits are typically used (Nansen, 2012), an important advantage of the regression fit in Eq. (2) is a very high level of regression convergence. That is, regression fits to variogram data are quite sensitive to the quality of the input data and will either not generate parameter coefficients or generate quite extreme coefficients (Isaaks and Srivastava, 1989). However using Eq. (2), it was possible to generate parameter coefficients for all 72 training data

sets and 30 validation data sets included in this study. Analysis of variance (PROC MIXED) was used to compare average variogram coefficients ( $a$ ,  $b$ , and  $c$ ) derived from the spectral band at 782 nm of non-infested and infested field pea samples.

Each of the LDAs was assessed based on its sensitivity (ability to accurately detect infestation), specificity (ability to accurately detect non-infestation), and the classification accuracy of the 30 independent validation data sets. The validation data were acquired with the same settings as for the training data set (64,000 pixels per hyperspectral image) and subjected to radiometric filtering (Eq. (1)) prior to independent validation analysis.

### 3. Results and discussion

The background color variability across the examined spectral range is represented by average reflectance profiles from the 24 field pea samples (Fig. 2a). The background color range (average maximum/average minimum) among non-infested field pea samples exceeded 3.5 in some spectral bands, and it was above 1.5 between 400 and 750 nm. It was within this considerable variability in background colors that we intended to determine whether it would be possible to detect a consistent reflectance response to pea weevil infestation. Each of the 72 hyperspectral images used to develop the classification model consisted of 2560 pixels or reflectance profiles ( $N = 184320$ ). After deploying Eq. (1), the input data set consisted of 108351 reflectance profiles. Based on stepwise discriminant analysis, we demonstrated that about 42% of the variance could be explained by a single spectral band, R782 (reflectance at 782 nm), and that the 20 spectral bands with highest contribution to the classification of field peas with/without pea weevil infestation all contributed up to 1% in terms of partial  $R^2$ -values (Fig. 2a). These 20 narrow spectral bands were used as explanatory variables in a LDA of the 108351 reflectance profiles, which were classified with a sensitivity of 84.5% and specificity of 83.7% (Table 1). This classification model was applied to the 30 independent validation data sets, which were classified with

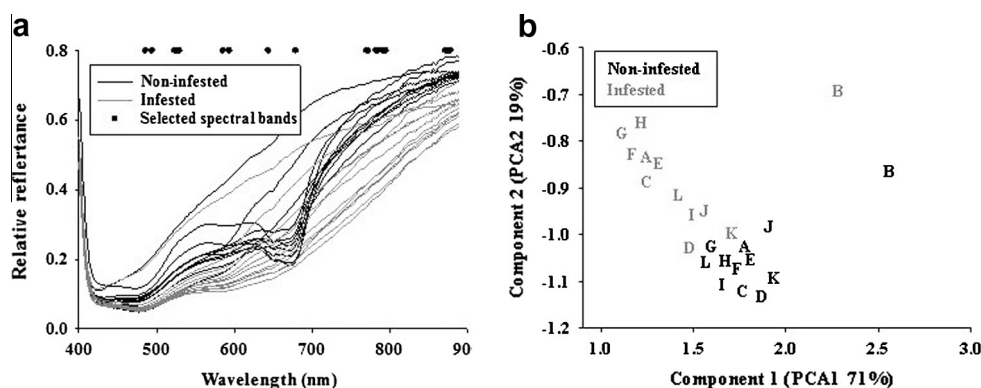


Fig. 2. Average reflectance profiles (a) and principal component analysis (b) of 12 field pea samples with/without pea weevil infestation. Letters A–L refer to the 12 field pea samples (see Fig. 1). Dots (a) represent the 20 spectral bands selected through stepwise linear discriminant analysis.

84.0% accuracy. We conducted the same linear discriminant analysis but used average reflectance in three spectral bands (694 nm, 877 nm, and 879 nm, which were selected from a stepwise LDA) as explanatory variables. Thus, the number of samples to be classified was reduced from 108351 to 72, and the sensitivity and specificity were 90.9% and 84.6%, respectively. In addition, the independent validation data were classified with 83.3% accuracy.

The 20 narrow spectral bands selected from the stepwise linear discriminant analysis were also used to conduct a principal component analysis (PCA), and average PCA scores were generated for each pea sample (Fig. 2b). The main purpose of conducting an unsupervised classification, like PCA, was to visualize inherent trends in the data set, and such trends can subsequently be used to develop accurate supervised classification methods. Pennant field peas were considerably lighter than the other field pea samples (“B” in Fig. 1), so they were also located quite far from the other pea samples within the two-dimensional space delineated by the two principal components (PCA1 and PCA2) (Fig. 2b). Despite the marked background color variability among pea samples, it was seen that pea weevil infestation caused a consistent change in reflectance profiles, as all pea samples showed a consistent shift in upwards-left direction in response to weevil infestation. Importantly, about 90% of the total variance was explained by the two principal components. Consequently, despite marked variability in background color of field peas, there was a consistent response

to pea weevil infestation, and it was well characterized by the two principal components. However, the PCA also showed that some of the non-infested pea samples (B6\_1, B11\_2, B8\_2, B10\_2, and Yarrum) and infested pea samples (B2\_4 and Kaspia) were located in a “transition zone” with poor separation between non-infested and infested field pea samples. These, pea samples would likely be difficult to accurately classify as either infested or non-infested, unless their relative background color (and therefore the relative shift in down-left direction) was somehow incorporated into the classification.

3.1. Linear discriminant analysis based on average reflectance and variogram parameters

The spectral band at 782 nm (R782) was chosen for variogram analysis, as it had the highest contribution to the separation of pixels acquired from non-infested and infested field peas. All three variogram parameters changed significantly in response to pea weevil infestation, especially *a* and *c* (Fig. 3a). Fig. 3b shows the change in spatial data structure (variograms) in three of the pea weevil samples in response to pea weevil infestation. These three examples were representative for the data included in this study and showed consistent increases in all three variogram parameters. Thus, it was highlighted that the three derived variogram parameters could be used as indicators of pea weevil infestation, and this is consistent with other studies, in which analyses of variance of individual variogram parameters have shown that these parameters can be used as indicators of biotic stress in plants (Nansen et al., 2010c). A LDA with the three variogram parameters as explanatory variables classified the 72 field pea samples with a sensitivity of 74.3% and a specificity of 73.0%, but the classification accuracy of independent validation samples was only 43.3% (Table 1). As indicated in the principal component analysis (Fig. 2b), it was believed that the mis-classification of some field pea samples was due to partial “classification overlap” due to the marked variability in background colors of field pea samples. Thus a second LDA was conducted, in which we included average reflectance values in two spectral bands (641 nm and 868 nm). The logic behind this approach was that reflectance values in these two spectral bands had been found to successfully capture the variability in background colors. Using the combination of these two spectral bands (representing the relative background color of field pea samples) and the three variogram parameters (*a*, *b*, and *c*), the 72 field pea samples were classified with a sensitivity of 94.7% and a specificity of 100.0% (Table 1). Consequently, the following linear discriminant functions are proposed for accurate classification of field pea samples:

Table 1 Classification results from linear discriminant analyses of reflectance data from field peas.

Assigned category		
Actual category	Non-infested	Infested
<i>Analysis of all 108,351 reflectance profiles</i>		
Non-infested	<b>43332 (82.3%)</b>	9328 (17.7%)
Infested	7923 (14.2%)	<b>47768 (85.8%)</b>
<i>Analysis of all 72 average reflectance profiles</i>		
Non-infested	<b>30 (83.3%)</b>	6 (16.7%)
Infested	3 (8.33%)	<b>33 (91.7%)</b>
<i>Only variogram parameters derived from R782 (72 samples)</i>		
Non-infested	<b>26 (72.2%)</b>	10 (27.8%)
Infested	9 (25.0%)	<b>27 (75.0%)</b>
<i>Variogram parameters from R782 and average reflectance (R641 and R868) (72 samples)</i>		
Non-infested	<b>36 (100.0%)</b>	0 (0.0%)
Infested	2 (5.6%)	<b>34 (94.4%)</b>

Classification results from four linear discriminant analyses with number and percentage of samples allocated to each of the two categories. Correctly classified samples are highlighted in bold.

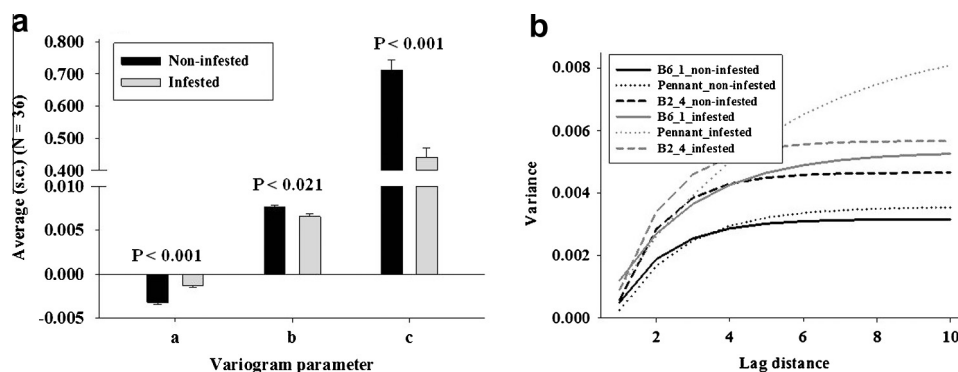


Fig. 3. Average variogram parameters (a) from non-infested and infested field pea samples and examples of variogram response to pea weevil infestation (b).

Non-infested :  $-406.16 - R641 \times 236.25 + 44277 \times a + 9769 \times b + 180.12 \times c$   
 Infested :  $-328.19 - R641 \times 202.37 + 47086 \times a + 12,199 \times b + 191.37 \times c$

The linear discriminant functions derived from the training data set from the 72 field pea samples was validated with reflectance data acquired from 30 independent hyperspectral images of field peas, and all 30 independent validation data sets were correctly classified (100.0%).

#### 4. Concluding remarks

Although reflectance-based technologies are widely and successfully used in both research and commercial production systems as part of product quality control and/or characterization of certain features in target objects, the performance of classification models is often severely reduced, when target objects vary considerably both within each object and between objects (i.e. varieties) in terms of color, size and shape. We believe that variability in physical characteristics of target objects represents one of the main challenges in future improvement of current trait classifiers based on reflectance data. Most analytical approaches address this challenge by developing classification methods that rely on high spectral resolution and/or fairly sophisticated (and computer-intensive) data processing and analysis. Such an approach with emphasis on sophistication means that classifications become comparatively expensive and also challenging to conduct in a timely manner. In this study, we demonstrated that LDA based on reflectance values in 20 narrow spectral bands provided higher classification accuracy (sensitivity and specificity) as classification based on three variogram parameters from a single spectral band. Thus, spatial information (quantitative information about the spatial structure) embedded in imaging data should be considered of considerable importance when developing reflectance based classifiers. Including two additional variables [the background color represented by average reflectance in two spectral bands (641 nm and 868 nm)] was associated with a sensitivity of 94.7% and a specificity of 100% and 100% accurate classification of independent validation data. Due to the accuracy and low amount of spectral data required to conduct the classification, we believe the combination of variogram parameters and average reflectance as explanatory variables is of considerable relevance to commercial quality control systems of a wide range of food products, in which data processing and analysis are required under significant time restrictions (i.e. when large amount of food items are moving on a conveyor belt).

#### References

Ariana, D.P., Renfu, L., 2010. Evaluation of internal defect and surface color of whole pickles using hyperspectral imaging. *Journal of Food Engineering* 96, 583–590.

- Aryamanesh, N., Byrne, O., Hardie, D.C., Khan, T., Siddique, K.H.M., Yan, G., 2012. Large-scale density-based screening for pea weevil resistance in advanced backcross lines derived from cultivated field pea (*Pisum sativum*) and *Pisum fulvum*. *Crop and Pasture Science* 63, 612–618.
- Byrne, O.M., Hardie, D.C., Khan, T.N., Speijers, J., Yan, G., 2008. Genetic analysis of pod and seed resistance to pea weevil in a *Pisum sativum* × *P. fulvum* interspecific cross. *Australian Journal of Agricultural Research* 59, 854–862.
- ElMasry, G., Wang, N., Vigneault, C., Qiao, J., ElSayed, A., 2008. Early detection of apple bruises on different background colors using hyperspectral imaging. *Food Science and Technology* 41, 337–345.
- Fisher, R.A., 1936. The use of multiple measurements in taxonomic problems. *Annals of Eugenics* 7, 179–188.
- Fontaine, J., Schirmer, B., Hörr, J., 2002. Near-infrared reflectance spectroscopy (NIRS) enables the fast and accurate prediction of essential amino acid contents. 2. Results for wheat, barley, corn, triticale, wheat bran/middlings, rice bran, and sorghum. *Journal of Agricultural and Food Chemistry* 50, 3902–3911.
- Gowen, A.A., O'Donnell, C.P., Cullen, P.J., Downey, G., Frias, J.M., 2007. Hyperspectral imaging – an emerging process analytical tool for food quality and safety control. *Trends in Food Science and Technology* 18, 590–598.
- Gowen, A.A., Taghizadeh, M., O'Donnell, C.P., 2009. Identification of mushrooms subjected to freeze damage using hyperspectral imaging. *Journal of Food Engineering* 93 (1), 7–12.
- Gcdmez-Sanchis, J., Gcdmez-Chova, L., Aleixos, N., Camps-Valls, G., Montesinos-Herrero, C., Molted, E., Blasco, J., 2008. Hyperspectral system for early detection of rotteness caused by *Penicillium digitatum* in mandarins. *Journal of Food Engineering* 89 (1), 80–86.
- Isaaks, E.H., Srivastava, R.M., 1989. *Applied Geostatistics*. Oxford University Press, New York, USA.
- Kalkan, H., Beriat, P., Yardimci, Y., Pearson, T.C., 2011. Detection of contaminated hazelnuts and ground red chili pepper flakes by multispectral imaging. *Computers and Electronics in Agriculture* 77 (1), 28–34.
- Kong, S.G., Chen, Y., Kim, I., Kim, M.S., 2004. Analysis of hyperspectral fluorescence images for poultry skin tumor inspection. *Applied Optics* 43, 824–832.
- Lefcote, A.M., Kim, M.S., 2006. Technique for normalizing intensity histograms of images when the approximate size of the target is known: detection of feces on apples using fluorescence imaging. *Computers and Electronics in Agriculture* 50, 135–147.
- Liu, L., Ngadi, M.O., Prasher, S.O., Garipey, C., 2010. Categorization of pork quality using Gabor filter-based hyperspectral imaging technology. *Journal of Food Engineering* 99 (3), 284–293.
- Lu, R., Peng, Y., 2006. Hyperspectral scattering for assessing peach fruit firmness. *Biosystems Engineering* 93, 161–171.
- Martens, M., Martens, H., 1986. Near-infrared reflectance determination of sensory quality of peas. *Applied Spectroscopy* 40, 303–310.
- Mehl, P.M., Chen, Y., Kim, M.S., Chan, D.E., 2004. Development of hyperspectral imaging technique for the detection of apple surface defects and contaminations. *Journal of Food Engineering* 61, 67–81.
- Nansen, C., 2011. Robustness of analyses of imaging data. *Optics Express* 19, 15173–15180.
- Nansen, C., 2012. Use of variogram parameters in analysis of hyperspectral imaging data acquired from dual-stressed crop leaves. *Remote Sensing* 4 (1), 180–193.
- Nansen, C., Abidi, N., Sidumo, A.J., Gharalari, A.H., 2010a. Using spatial structure analysis of hyperspectral imaging data and fourier transformed infrared analysis to determine bioactivity of surface pesticide treatment. *Remote Sensing* 2, 908–925.
- Nansen, C., Herrman, T., Swanson, R., 2010b. Machine vision detection of bonemeal in animal feed samples. *Applied Spectroscopy* 64 (6), 637–643.
- Nansen, C., Kolomiets, M., Gao, X., 2008. Considerations regarding the use of hyperspectral imaging data in classifications of food products, exemplified by analysis of maize kernels. *Journal of Agricultural and Food Chemistry* 56 (9), 2933–2938.
- Nansen, C., Macedo, T., Swanson, R., Weaver, D.K., 2009. Use of spatial structure analysis of hyperspectral data cubes for detection of insect-induced stress in wheat plants. *International Journal of Remote Sensing* 30 (10), 2447–2464.

- Nansen, C., Sidumo, A.J., Capareda, S., 2010c. Variogram analysis of hyperspectral data analysis to characterize impact of biotic and abiotic stress of maize plants and to estimate biofuel potential. *Applied Spectroscopy* 64 (6), 627–636.
- Okamoto, H., Lee, W.S., 2009. Green citrus detection using hyperspectral imaging. *Computers and Electronics in Agriculture* 66, 201–208.
- Park, B., Lawrence, K.C., Windham, R.W., Smith, Douglas P., 2006. Performance of hyperspectral imaging system for poultry surface fecal contaminant detection. *Journal of Food Engineering* 75, 340–348.
- Park, B., Yoon, S.C., Lawrence, K.C., Windham, W.R., 2007. Fisher linear discriminant analysis for improving fecal detection accuracy with hyperspectral images. *Transactions of the ASABE* 50 (6), 2275–2283.
- Shahin, M.A., Symons, S.J., 2011. Detection of fusarium damaged kernels in canada western red spring wheat using visible/near-infrared hyperspectral imaging and principal component analysis. *Computers and Electronics in Agriculture* 75 (1), 107–112.
- Vargas, A.M., Kim, M.S., Yang, T., Lefcourt, A.M., Chen, Y.-R., Luo, Y., Song, Y.R.B., 2005. Detection of fecal contamination on cantaloupes using hyperspectral fluorescence imagery. *Journal Food Science* 70, 471–476.
- Wang, W., Paliwal, J., 2007. Near-infrared spectroscopy and imaging in food quality and safety. *Sensing and Instrumentation for Food Quality and Safety* 1, 193–207.